EuroIntervention 2012;7:1444-1452

Characterisation of a novel porcine coronary artery CTO model

Paul Fefer[1,4], MD; Normand Robert[2], PhD; Beiping Qiang[1], MD; Garry Liu[2], BASc, MSc; Nigel Munce[2], PhD; Kevan Anderson[2], PhD; Azriel B. Osherov[1], MD; Michelle Ladouceur-Wodzak[1]; Xiuling Qi[2], PhD; Alexander Dick[1,2], MD; Max Weisbrod[1]; Michelle Samuel[1]; Jagdish Butany[3], MD; Graham Wright[1,2], PhD; Bradley H. Strauss[1]*, MD, PhD

1. Division of Cardiology, Schulich Heart Centre, Sunnybrook Health Sciences Centre, Toronto, Ontario, Canada; 2. Imaging Research, Departments of Medicine and Medical Biophysics, Sunnybrook Health Sciences Centre, Toronto, Ontario, Canada; 3. Department of Pathology, University Health Network, University of Toronto, Toronto, Canada; 4. Heart Center, Sheba Medical Center, Tel Hashomer, Israel and Sackler Faculty of Medicine, Tel Aviv University, Tel Aviv, Israel

KEYWORDS

- chronic total occlusion
- coronary arteries
- animal model
- pathology
- neovessels

Abstract

Aims: To create a large animal coronary chronic total occlusion (CTO) model. Presence of microvessels within the CTO lumen facilitates guidewire crossing. The patterns and time profiles of matrix changes and microvessel formation during coronary CTO maturation are unknown.

Methods and results: CTO were created in 15 swine by percutaneous deployment of a collagen plug. Matrix changes were assessed by histology. Intraluminal neovascularisation was assessed by histology and several imaging modalities, including conventional and 3D spin angiography, micro-computed tomography (micro-CT) imaging, and contrast-enhanced magnetic resonance imaging (MRI), at six and 12 weeks following CTO creation. Matrix changes included an intense inflammatory reaction at six weeks which had partially abated by 12 weeks. A proteoglycan-rich matrix at six weeks was partially replaced with collagen by 12 weeks. Similar changes were noted in the proximal cap which was acellular. Three patterns of microvessel formation were identified and defined based on the presence and extent of a "lead" neovessel. No major differences in pattern or extent of neovascularisation were noted between six and 12 weeks.

Conclusions: Heterogeneity in neovascularisation patterns occurs during coronary CTO development in a porcine model. Non-invasive imaging to determine the predominant type of neovascularisation prior to and during CTO revascularisation may improve guidewire crossing success rates. This model may be useful for further exploration of CTO pathophysiology, and may aid in further refinements of *in vivo* imaging of CTO and development of novel therapeutic approaches to revascularisation of CTO, such as manipulations of the proximal cap, matrix composition, neovessel induction, and device testing.

**Corresponding author: Schulich Heart Program, Sunnybrook Health Sciences Centre, Room A-253, 2075 Bayview Avenue, Toronto, Ontario, M4N 3M5, Canada. E-mail: Bradley.strauss@sunnybrook.ca*

© Europa Edition 2012. All rights reserved.

DOI: 10.4244/EIJV7I12A225

Introduction

Chronic total occlusions (CTO) in coronary circulation are associated with significant morbidity and adverse outcomes[1,2]. They remain a significant challenge to the interventional cardiologist with success rates of 55-80%[3,4], primarily due to failure of guidewire crossing through the occlusion[2,5,6]. Neovascularisation of the CTO lumen may constitute an important aspect of the maturation process. Previous studies of human arteries and experimental CTO have suggested that the presence of microvessels within the CTO lumen may facilitate guidewire crossing, either as a direct pathway or by enhancing favourable changes in the composition of the surrounding matrix[7,8]. We have recently reported our analysis of compositional changes occurring during CTO maturation in a rabbit model[9]. However, this work was done in a rabbit peripheral (femoral) artery model, which may develop quite differently than coronary artery CTO. The objective of this study was to create a large animal coronary CTO model that would closely emulate human coronary CTO and to characterise microvessel formation and matrix maturation at two time points after CTO creation. Both vascular and non-vascular changes were assessed using an approach that combined histology, specific matrix and calcium stains, and complementary *in vivo* and *ex vivo* imaging.

Methods

THE OCCLUSION MODEL

Animal experiments conformed to the "Position of the American Heart Association on Research Animal Use." Approval for experiments was obtained from St. Michael's and Sunnybrook Hospital Animal Care Committees (both Toronto, Canada). Coronary occlusions were performed in 27 female Yorkshire swine (25-30 kg). Animals were treated with a beta blocker (atenolol 25 mg/d), orally, beginning seven days prior to the procedure and continued until sacrifice. Anaesthesia was induced using xylazine 1-2 mg/kg and ketamine (30 mg/kg) and after intubation, anaesthesia was maintained with inhaled isofluorane 1-4%. Cutdown of the right carotid artery was performed and an 8 Fr sheath was inserted, followed by administration of 5,000 IU of unfractionated heparin (APP Pharmaceuticals, Schaumburg, IL, USA). Under fluoroscopic guidance, cannulation of the left main coronary artery was performed using a 7 Fr Judkins Left (JL) 3.5 guiding catheter (Cordis Corp., Miami Lakes, FL, USA). A 5 Fr multipurpose guiding catheter, which was preloaded at the tip with a collagen plug (Angio-Seal®, St. Jude Medical, St. Paul, MN, USA), was advanced through the guiding catheter and positioned in the mid left anterior descending artery (LAD). The collagen plug was then advanced outside the 5 Fr catheter with the simultaneous use of two 0.035 inch guidewires. The 5 Fr catheter was removed and the mid LAD occlusion was confirmed by angiography, after which all equipment was removed, the carotid artery was sutured and the incision closed. The animal was monitored for ventricular arrhythmias over a 60 minute period. The coronary artery occlusion technique is shown in **Figure 1**.

Animals with ventricular ectopy were treated with intravenous lidocaine (1-2 mg/kg) and amiodarone (75 mg bolus injection), and defibrillation, if necessary. After 60 minutes following the procedure, animals were recovered and returned to their pens. Buprenorphine 0.01-0.02 mg/kg (IM) was given routinely for post-procedural pain management. The pigs were fed a regular chow diet. Angiographic follow-up and sacrifice were performed at six weeks in 11 pigs and at 12 weeks in seven pigs. Angiography was performed using a 6 Fr JL 3.5 diagnostic catheter. Animals in which a CTO was confirmed (total or subtotal occlusion with Thrombolysis In Myocardial Infarction (TIMI) grade 0-1 flow distal to the occlusion) were included in the analysis. After angiography, the animals were taken for cardiac MRI. After completion of *in vivo* imaging studies (angiography and MRI), euthanasia was performed under general anaesthesia by IV injection of pentobarbital euthanasia solution (100 mg/kg). The heart was excised and the coronary arteries were flushed with lactated Ringer's solution and then injected with Microfil® (Flowtech, Carver, MA, USA). **Figure 2** shows angiograms of the LAD at different time points before and after creation of occlusion.

MRI

The MRI studies were performed on a 3T GE Excite™ Scanner (GE Healthcare, Milwaukee, WI, USA) by the use of a custom (5×3 cm) surface coil secured over the chest. Occlusions were

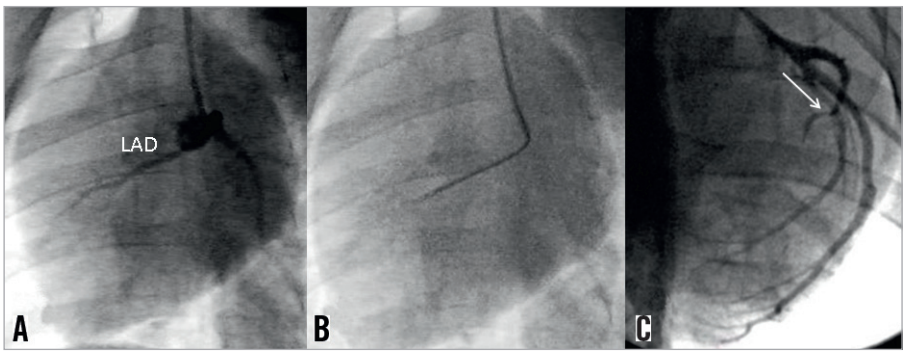

Figure 1. *Coronary artery occlusion technique. A) Angiogram of the LAD before intervention; B) 5 Fr catheter telescoped into the mid-LAD; and C) shows the occluded LAD after Angio-Seal® deployment (arrow).*

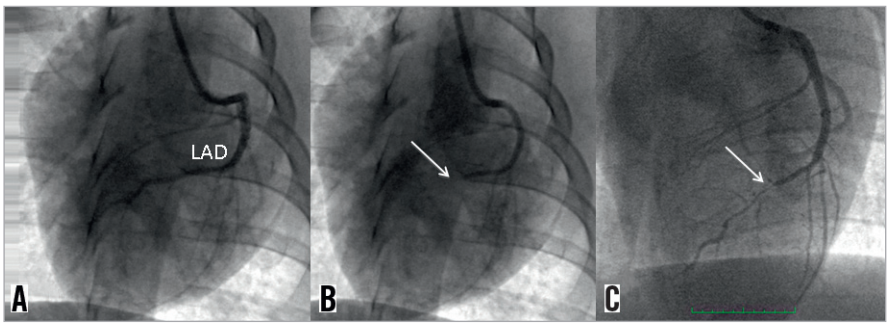

Figure 2. *Angiogram of the LAD before, immediately post-, and six weeks post-occlusion. A) Preprocedural angiogram of the LAD; B) Immediate post-procedure completely occluded LAD (arrow); and C) 6-week angiogram with small revascularisation channel through the occluded segment (arrow).*

imaged with the use of an elliptic-centred fast spoiled gradient echo sequence (repetition time/echo time=8.3/2.1/30°, 31.25 kHz receive bandwidth, resolution of 0.25 mm in plane, 0.6 mm through plane). The elliptic ordering of acquisition procures most of the contrast during the first several seconds and, thus, the images are more representative of the contrast close to the start of the imaging.

T1-weighted images were obtained 16 sec after the injection of 0.05 ml/kg Clariscan™ (Feruglose; GE Healthcare, Chalfont, UK). To maintain an adequate signal-to-noise ratio, each data point was consecutively averaged four times, yielding an imaging time of 216 sec. Clariscan™ (Nycomed Imaging, Oslo, Norway) remains intravascular and reflects relative blood volume (RBV) within the CTO lumen[10,11] serving as a surrogate for perfusion. Regions of interest were selected in the proximal part of the CTO from each of the T1-weighted MR images to calculate average signal intensity. Relative distribution volume of Clariscan was derived from the ratio of tissue signal intensity in the region of interest compared with the vessel segment immediately proximal to the CTO[12].

3D SPIN ANGIOGRAPHY AND CT

Intravenous heparin (5,000 IU) was administered to the animals before they were sacrificed to prevent blood coagulation in the microvasculature. The heart was excised and 30 ml Microfil was injected selectively into the coronary arteries at a pressure of 90 mm Hg, as measured by a handheld manometer and stored in saline. The hearts were imaged within 1-3 days on an Innova® 2121IQ (GE Healthcare, Buc, France [GEHC]) catheterisation system in spin mode resulting in the acquisition of 146 frames in 4.8 sec at 60 kVp, 150-250 mA with 6 msec pulse/frame, with a 190 degree gantry rotation. Reconstruction from the projection data was done on an Advantage Workstation™ (GEHC), resulting in a reconstructed volume with voxels of (0.23 mm)[13] in size. CT was also performed with a GEHC LightSpeed® scanner at 140 kVp, 500-775 mA for 7.5 sec yielding a reconstructed volume with a voxel size of 0.28 mm×0.28 mm×0.62 mm and a slice spacing of 0.38 mm. Volume-rendered sequences of images from varying perspectives were generated from the CT and Innova reconstructions providing 3D perception of the vascular structures.

MICRO-CT IMAGING

The coronary arteries were fixed in formalin for 48 hrs, embedded in 1% w/w agarose gel, and imaged on a micro-CT (MS-8; GE Medical Systems, London, Ontario, Canada), having a 14 µm detector pixel size. A total of 905 cone beam projection images spanning 360 degrees were acquired with an equivalent pixel size of 28 µm at 80 kVp, 90 µA (540 µAs per projection) in 2.5 hours. A 3-dimensional data set was reconstructed with a voxel size of 54 µm using the scanner's implementation of the Feldkamp reconstruction algorithm. A subset of the volume encompassing the occlusion or stenosis was also reconstructed at a smaller voxel size of 28 µm. Images were exported into Amira® (Mercury Computer Systems, Chelmsford, MA, USA) as series of axial slices and were volume-rendered by setting the threshold slightly higher than the Hounsfield units of the Microfil to display the vasculature.

Figure 3 shows the various imaging techniques used for vessel analysis.

HISTOLOGICAL ANALYSIS

After micro-CT imaging, the proximal occluded segment containing the proximal fibrous cap was cut into sequential 0.5 mm longitudinal sections, while the distal segment was cut into sequential 2 mm cross-sections throughout the length of the occluded segment. Sections were stained with haematoxylin and eosin and Movat pentachrome stains. Representative von Kossa stains were also obtained to assess the presence of calcium. The proximal and distal CTO segments were defined as the sections within the CTO that were immediately adjacent to the patent artery at the entry and exit sites, respectively. All other sections were defined as the body of the CTO. The CTO microvessels within the occluded lumen were identified on Movat-stained sections as vascular structures lined with endothelial cells, and typically were filled with Microfil. In some cases, red blood cells also were evident.

Results

A total of 26 pigs underwent LAD total occlusion creation. Of these, 17 survived till planned sacrifice. Of the nine pigs that died, two died of procedure-related events (difficult intubation and aortic

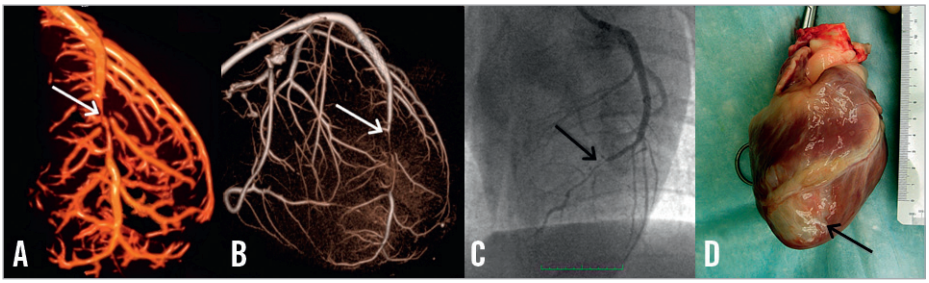

Figure 3. *Various imaging techniques used for vessel analysis. A) 3D reconstruction of an ex vivo CT scan on excised heart after Microfil; B) 3D spin angiogram performed on excised heart after Microfil; C) standard pre-sacrifice angiogram; D) Gross pathology of the excised heart. Black arrow shows white scar tissue at the left ventricular apex corresponding with a mid-LAD infarct.*

dissection after failed attempts to cannulate an aberrant left main artery, respectively), and seven died suddenly between two hours to two weeks after the procedure (almost all deaths were within 12 hours). In two of the 17 pigs that survived the procedure, we failed to create an occlusion, and these pigs were excluded from further analysis. Full analyses were performed on 15 pigs (eight pigs at the six-week time point and seven pigs at the 12-week time point).

Three patterns of microvessel formation were identified by micro-CT analysis and 3D spin angiography in the experimental coronary CTOs as follows:

1) Type 1 denotes the presence of a predominant "lead" neovessel vessel traversing the full length of the occluded segment **(Figure 4A and Figure 5A)**, and creating a partially recanalised occlusion.
2) Type 2 denotes the presence of a lead neovessel which does not traverse the full length of the occluded segment **(Figure 4B and Figure 5B)**.
3) Type 3 denotes the lack of a lead neovessel **(Figure 4C and Figure 5C)**.

In all three types, discontinuous microvessels of variable diameter and vessel density were common throughout the occluded segment.

At six weeks, the majority of the pigs (five out of eight pigs) demonstrated a type I recanalisation pattern, while one pig occlusion was of type II and two occlusions were type III. At 12 weeks, five CTO were type I, two CTO were type II and none were type III. Lead neovessels were common in both six-week and 12-week CTO. Of note, the presence and extent of small microvessels was variable between pigs, but no major differences were observed at 12-week compared to six-week CTO. Moreover, the content of proteoglycan and collagen was variable between animals but again, no discernible differences were noted at 12-week compared to six-week CTO.

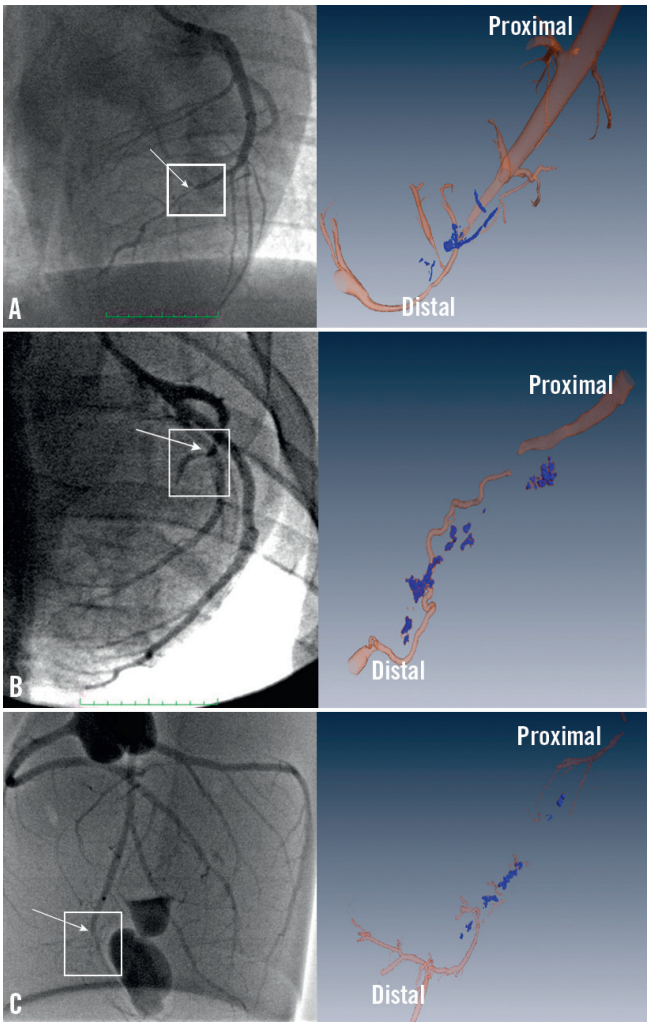

Figure 4. *Angiogram (left panels) and volume rendered micro-CT reconstruction (right panels) of occluded coronary arteries. A) type I; B) type II; C) type III. The square over the angiogram marks the area of interest shown in the micro-CT image. The arrows show the proximal occlusion point. Note large neovessel traversing the whole length of the CTO in type I CTO; a discontinuous neovessel in type II; and lack of lead neovessel in type III.*

PROXIMAL CAP

Proximal caps were available for analysis for three pigs (two six-week pigs and one 12-week pig). Neovessels were not noted at the proximal cap region in these samples. The proximal cap at six

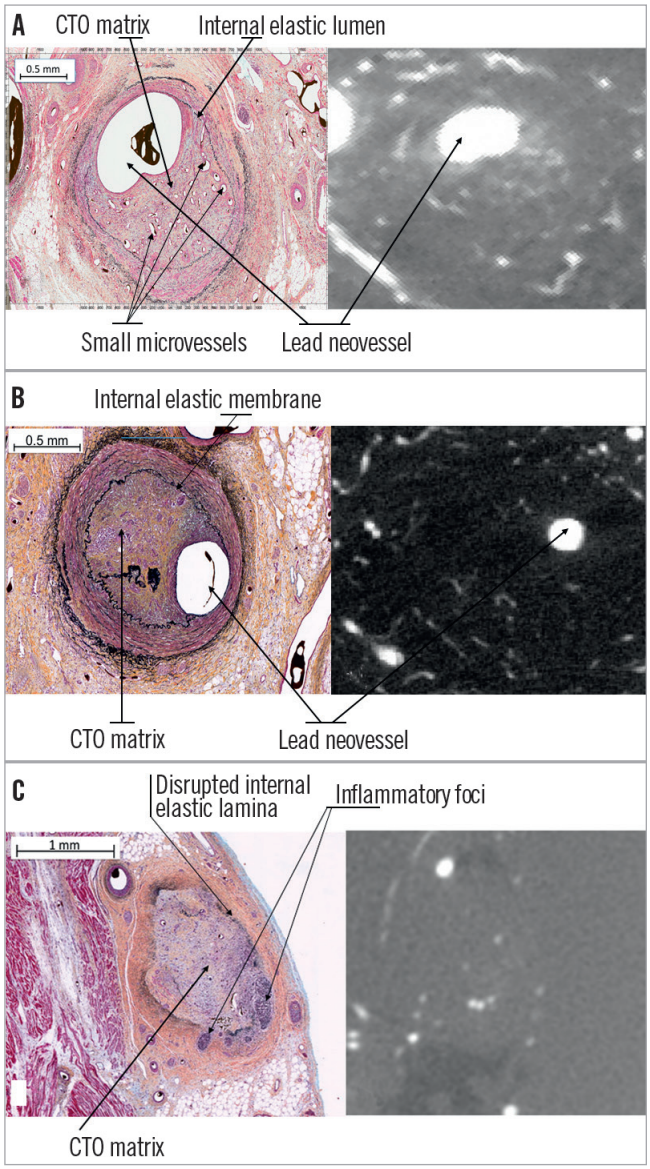

Figure 5. *Histology at a mid-occlusion level (Movat stain) (left panels) and corresponding micro-CT image (right panels) of occluded coronary arteries. A) type I; B) type II; C) type III. Note the large neovessel (maximal diameter 500-1300 microns) in type I and type II occlusions and lack of a lead neovessel in type III. Note also numerous small microvessels in panel and matrix composed of a mixture of collagen (stained brown) and proteoglycan (stained blue) evident in (B). Panel c also shows disruption of the internal elastic lamina and numerous foci of inflammation.*

weeks was highly cellular with a proteoglycan-rich matrix and absence of microvessels in the initial 1.5 mm at the entry **(Figure 6A)**. Distal to the cap, there was some disruption of the integrity of the internal elastic lamina (IEL). The matrix in this region was a mixture of proteoglycans and collagen. The proportion of collagen became progressively higher in the distal direction of the occlusion. Microvessels were apparent about 2 mm within the proximal cap, within the collagen-rich matrix. A large focus of necrosis and inflammatory cells was evident along with positive remodelling and IEL disruption (arrow). This finding seems to be associated with a specific inflammatory reaction to the fibrin plug. At 12 weeks **(Figure 6B)**, in contrast to the six-week histology, the proximal cap was a fibrotic, nearly acellular structure, with a predominantly densely packed collagen- and elastin-rich matrix with minimal proteoglycan. Similar to the six-week proximal cap, microvessels were also not present in the very proximal part of the cap, but appeared to originate about 1.5 mm distally.

PRESENCE OF CALCIUM

Calcium was evident already in the six-week occlusion specimens and was corroborated by calcium-specific stains. Calcium was seen predominantly in the central necrotic core of the occlusion **(Figure 7A)**. At 12 weeks, calcium deposits were more abundant than at the earlier time point, although still predominantly in the central necrotic core **(Figure 7B)**.

Discussion

In this study we describe a novel porcine coronary CTO model and provide detailed characterisation of neovessel formation and matrix maturation at two time points. Using advanced *in vivo* and *ex vivo* imaging techniques we identified three patterns of microvessel formation within coronary CTO, based on the presence and extent of a lead neovessel. We also defined the histological appearance and maturation of the proximal cap and of the extracellular matrix at six and 12 weeks post-CTO creation.

We have previously analysed compositional changes in arterial CTO in a rabbit model[9]. This study extends the findings of our previous model to a large animal coronary CTO, which more closely emulates a human coronary CTO. In this study we specifically concentrated on large neovessel formation within the CTO, in addition to characterising temporal changes in the proximal fibrous cap and the extracellular matrix composition. We will discuss these topics separately.

THROMBUS, INFLAMMATION, AND NEOVESSEL FORMATION

Similar to our previous rabbit model, CTO creation was secondary to non-atherosclerotic thrombotic occlusion of the artery with subsequent inflammation, thrombus organisation and neovascular formation. There are few published data on the process of microvessel formation in arterial thrombi but inflammation seems to be central to the process of neovascularisation[14,15]. In the rabbit model, inflammation was most intense at two weeks post-CTO creation and progressively abated by the 12- and 18-24 week time points. In the current study we had only two time points, six weeks and 12 weeks post-CTO formation. The six-week occlusions demonstrated an intense inflammatory reaction with prominent macrophage infiltration, which was still present, though less intense, at 12 weeks. Previous studies have similarly shown high concentrations of macrophages in regions of recanalisation in spontaneous human

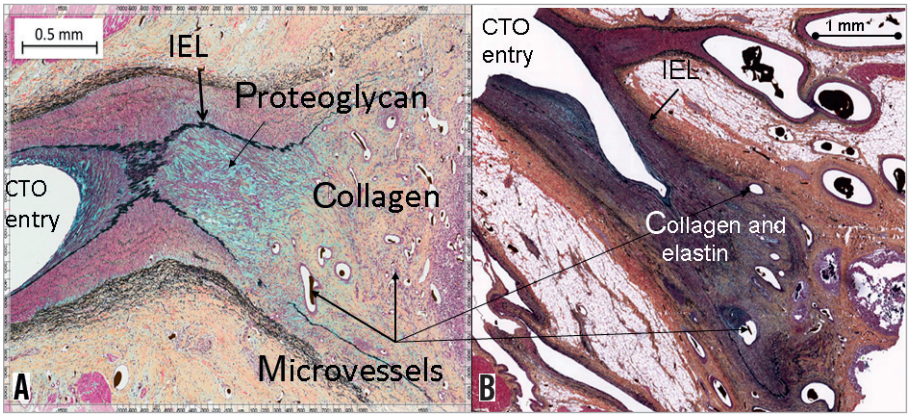

Figure 6. *Histology of the proximal cap (Movat stains) at two time points. A) Proximal cap at 6 weeks; B) Proximal cap at 12 weeks. Note the predominance of cellular elements and proteoglycan (stained blue) in the six-week cap versus the predominance of dense collagen and elastin (stained brown and black respectively) in the 12-week cap.*

thrombi and in experimental animal arterial thrombi[16,17]. Srivatsa et al[7] likewise reported that microvessel content in human coronary CTO correlated with the degree of inflammation. Our study is in line with these data and supports the association between the intense inflammatory reaction and the presence of neovessels. However, in the rabbit peripheral arterial model[9], there was a progressive reduction with time in the inflammatory response that was accompanied by a reduction in microvessel cross-sectional area and relative blood volume (both are measures of neovessel concentration). In our study, lead neovessels were at least as prominent at 12 weeks as they were at six weeks, which may be due to the presence of significant inflammation noted at both time points in this model. The neovessels took a serpentine course through the obstructed section and often demonstrated a corkscrew-like appearance consistent with the process of new vessel formation and not simply native vessel recanalisation (e.g., **Figure 4B**).

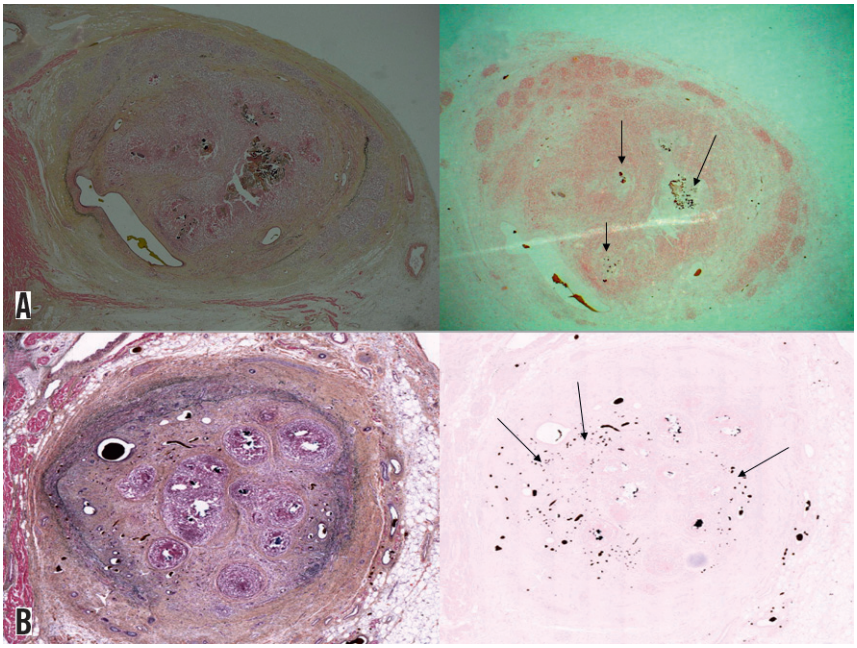

Figure 7. *Calcification increased at 12 weeks compared to the six-week-old CTO. A) Six-week CTO cross-section; B) 12 weeks post-CTO induction (left panels are Movat stains; right panels are von Kossa stains for calcium). Note presence of calcium (arrows on right panels) within the necrotic cores evident on the Movat stained specimen on left panel A (Microfil within the microvessels, as well as calcium in the tissue, appears dark on von Kossa stains. Calcium deposits have more jagged edges and calcium appears purplish on the Movat stain, whereas the Microfil remains black.*

PATTERNS OF NEOVESSEL FORMATION

We identified three forms of lead microvessel formation: type I, characterised by a lead neovessel that traverses the full length of the CTO, creating a partially recanalised occlusion; type II, where the lead neovessel is present but discontinuous; and type III, no lead neovessel is present. There are two potentially important consequences of microvascular formation. First, neovascularisation might enable some perfusion distal to the occlusion which could potentially preserve viability in the distal vascular bed, provided the neovessels developed prior to complete vessel occlusion. Second, partial recanalisation of the CTO with large neovessels (500-1000 micron diameter) such as seen in type 1 CTO may facilitate successful guidewire (360 micron diameter) crossing through the occlusion[7,8,18]. However, this type of neovessel is unlikely to be common in well-established human CTO and it is more likely that the presence of multiple, even discontinuous, microvessels along with specific matrix composition, may create a looser tissue, enabling loose tissue tracking by coronary guidewires. In our previous study in rabbit femoral arteries, there was a marked decline in intraluminal microvessel formation between six and 12 weeks, unlike the findings in this porcine model. Another notable difference was the positive remodelling of the occluded segments both at six-weeks and at 12-weeks post-CTO induction, which was in contrast to the marked vessel shrinkage observed in the rabbit model. These changes are likely due to a persistent inflammatory response in the pig model whereas by 12 weeks the inflammatory response had abated in the rabbit model. This prolonged inflammatory response may be due to the effects of a persistent collagen plug or the time frame of maturational changes may be different in the two species. Additional factors that may be involved include differences in the rheology and fibrinolytic systems[19,20].

PROXIMAL CAP AND MATRIX

In our rabbit peripheral artery CTO model[9] we described changes in the extracellular matrix composition of the occlusion over time. Similar to our previous findings, six-week occlusions demonstrate a proteoglycan-rich matrix with a prominent inflammatory reaction. At 12 weeks, the inflammatory reaction had declined, and the proteoglycan content was replaced with a predominantly collagen-rich matrix. While similar findings were observed in the pig model, matrix maturation seemed to evolve more slowly in the pig model compared with the rapid changes observed in the small animal model. Likewise, we defined histologically the maturation of the proximal cap. At six weeks **(Figure 6A)** the cap was characterised by a proteoglycan- rich matrix with highly cellular content and no microvessels in the proximal 1.5 mm of the occlusion. The matrix in this region was a mixture of proteoglycans and collagen with progressively higher collagen content observed distally. At 12 weeks, similar to the changes observed in the CTO body, examination of the proximal cap demonstrated a predominantly collagen- and elastin-rich matrix with very little proteoglycan. At both time points, the first 1-1.5 mm of the cap were avascular with microvessels appearing further distally.

This study represents the first description of temporal changes in the proximal cap region in a coronary occlusion model. These compositional changes with increased collagen content in the cap region support a biological basis for the clinical observation of increased guidewire failure to cross older CTO.

RELEVANCE TO HUMAN CTO

Although CTO are common and difficult to treat with percutaneous coronary intervention (PCI), data from human pathological studies are sparse and anecdotal. A relevant animal model is necessary for systematic analysis of the process of CTO maturation and for the development of innovative therapeutic approaches. Our model recreates many features that have been recognised in the natural history of CTO maturation[1] in that it is a large animal coronary occlusion model, including an initial thrombotic occlusion, acute inflammatory response, and the presence of calcium, microvessels and collagen-rich fibrous tissue. Numerous endoluminal approaches have been used in an attempt to mimic human CTO in an animal model including balloon-induced vessel wall injury[21], copper stent implantation[22], and thermal injury[23]. An earlier model from our group utilised local application of liquid thrombin[24]. These models were partially successful in reproducing mature fibrous tissue, an inflammatory reaction, neointimal proliferation, and small intraluminal channels within the CTO. A recently reported model succeeded in reproducing calcification within the CTO[25]. However, this model utilised implantation of bone chips along with an absorbable gelatine sponge. Our model is unique in that it demonstrates many of the findings observed in human coronary CTO, including the spontaneous appearance of calcification, developing subsequent to an acute thrombotic occlusion of the coronary artery. The process of calcification observed here is likely related to the intense inflammatory reaction and may be similar to that which occurs in native CTO. Our study is the first to define and categorise large neovessel formation over time. Of particular importance, the detailed microvessel imaging from the complementary imaging modalities used in our study were closely correlated with the histological data. Further refinements of these imaging techniques, particularly when applied by non-invasive or minimally invasive approaches, should be very useful for selecting patients likely to be successfully revascularised and to indicate cases that will need additional facilitating therapies such as plaque softening agents like collagenase[24]. Future studies to characterise later time points should also be considered to determine whether the differences between rabbit and pig models are only time-related changes.

Limitations

The CTO creation in this model was secondary to non-atherosclerotic thrombotic occlusion of a coronary artery with subsequent inflammation, thrombus organisation and neovascular formation along with the undesirable creation of a myocardial infarction. This is likely different from the development of many CTO in humans in which pre-existing collaterals are able to preserve the related myocardium despite complete epicardial vessel occlusion. Another limi-

tation is the short CTO maturation time (up to 12 weeks), which is obviously much less than most CTO observed in clinical practice.

In summary, we have developed a large animal model of calcified coronary CTO that mimics various aspects of human coronary CTO. The heterogeneity of this model in terms of the microvascular maturational changes is potentially very useful for imaging refinements to improve lesion characterisation as well as testing new therapeutic approaches, including devices and possible ways to modify vascular and/or matrix composition to enable successful revascularisation. The decision to pursue revascularisation of a CTO should be based on clinical data and the presence of viable myocardium in the CTO territory.

Funding

Supported by a Grant from the Canadian Institute of Health Research (Grant # CTP 82943).

Conflict of interest statement

The authors have no conflicts of interest to declare.

References

1. Stone GW, Kandzari DE, Mehran R, Colombo A, Schwartz RS, Bailey S, Moussa I, Teirstein PS, Dangas G, Baim DS, Selmon M, Strauss BH, Tamai H, Suzuki T, Mitsudo K, Katoh O, Cox DA, Hoye A, Mintz GS, Grube E, Cannon LA, Reifart NJ, Reisman M, Abizaid A, Moses JW, Leon MB, Serruys PW. Percutaneous recanalization of chronically occluded coronary arteries: a consensus document: part I. *Circulation*. 2005;112: 2364-72.

2. Srinivas VS, Brooks MM, Detre KM, King SB 3rd, Jacobs AK, Johnston J, Williams DO. Contemporary Percutaneous Coronary Intervention Versus Balloon Angioplasty for Multivessel Coronary Artery Disease: A Comparison of the National Heart, Lung and Blood Institute Dynamic Registry and the Bypass Angioplasty Revascularization Investigation (BARI) Study. *Circulation*. 2002;106:1627-1633.

3. Suero JA, Marso SP, Jones PG, Laster SB, Huber KC, Giorgi LV, Johnson WL, Rutherford BD. Procedural outcomes and long-term survival among patients undergoing percutaneous coronary intervention of a chronic total occlusion in native coronary arteries: a 20-year experience. *J Am Coll Cardiol*. 2001;38:409-14.

4. Safian RD, McCabe CH, Sipperly ME, McKay RG, Baim DS. Initial success and long-term follow-up of percutaneous transluminal coronary angioplasty in chronic total occlusions versus conventional stenoses. *Am J Cardiol.* 1988;61:23G-28G.

5. Puma JA, Sketch MH Jr, Tcheng JE, Harrington RA, Phillips HR, Stack RS, Califf RM. Percutaneous revascularization of chronic coronary occlusions: an overview. *J Am Coll Cardiol*. 1995;26:1-11.

6. Prasad A, Rihal CS, Lennon RJ, Wiste HJ, Singh M, Holmes DR Jr. Trends in outcomes after percutaneous coronary intervention for chronic total occlusions: a 25-year experience from the Mayo Clinic. *J Am Coll Cardiol*. 2007;49:1611-8.

7. Srivatsa SS, Edwards WD, Boos CM, Grill DE, Sangiorgi GM, Garratt KN, Schwartz RS, Holmes DR Jr. Histologic correlates of angiographic chronic total coronary artery occlusions: influence of occlusion duration on neovascular channel patterns and intimal plaque composition. *J Am Coll Cardiol*. 1997;29: 955-63.

8. Strauss BH, Segev A, Wright GA, Qiang B, Munce N, Anderson KJ, Leung G, Dick AJ, Virmani R, Butany J. Microvessels in chronic total occlusions: pathways for successful guidewire crossing? *J Interv Cardiol*. 2005;18:425-36.

9. Jaffe R, Leung G, Munce NR, Thind AS, Leong-Poi H, Anderson KJ, Qi X, Trogadis J, Nadler A, Shiff D, Saperia J, Lockwood J, Jacobs C, Qiang B, Teitelbaum A, Dick AJ, Sparkes JD, Butany J, Wright GA, Strauss BH.. Natural history of experimental arterial chronic total occlusions. *J Am Coll Cardiol*. 2009;53: 1148-58.

10. Kellar KE, Fujii DK, Gunther WH, Briley-Saebø K, Bjørnerud A, Spiller M, Koenig SH. NC100150 injection, a preparation of optimized iron oxide nanoparticles for positive-contrast MR angiography. *J Magn Reson Imaging*. 2000;11:488-94.

11. Bjornerud A, Johansson LO, Briley-Saebo K, Ahlstrom HK. Assessment of T1 and T2* effects in vivo and ex vivo using iron oxide nanoparticles in steady state– dependence on blood volume and water exchange. *Magn Reson Med.* 2002;47:461-71.

12. Schwarzbauer C, Syha J, Haase A. Quantification of regional blood volumes by rapid T1 mapping. *Magn Reson Med*. 1993;29: 709-12.

13. Marxen M, Thornton MM, Chiarot CB, Klement G, Koprivnikar J, Sled JG, Henkelman RM. Micro-CT scanner performance and considerations for vascular specimen imaging. *Med Phys*. 2004;31:305-13.

14. Heil M, Ziegelhoeffer T, Pipp F, Kostin S, Martin S, Clauss M, Schaper W. Blood monocyte concentration is critical for enhancement of collateral artery growth. *Am J Physiol Heart Circ Physiol*. 2002;283:H2411-9.

15. Doyle B, Caplice N. Plaque neovascularization and antiangiogenic therapy for atherosclerosis. *J Am Coll Cardiol.* 2007;49:2073-80.

16. McGuinness CL, Humphries J, Waltham M, Burnand KG, Collins M, Smith A. Recruitment of labelled monocytes by experimental venous thrombi. *Thromb Haemost*. 2001;85:1018-24.

17. Singh I, Burnand KG, Collins M, Luttun A, Collen D, Boelhouwer B, Smith A. Failure of thrombus to resolve in urokinase-type plasminogen activator gene-knockout mice: rescue by normal bone marrow-derived cells. *Circulation*. 2003;107:869-75.

18. Katsuragawa M, Fujiwara H, Miyamae M, Sasayama S. Histologic studies in percutaneous transluminal coronary angioplasty for chronic total occlusion: comparison of tapering and abrupt types of occlusion and short and long occluded segments. *J Am Coll Cardiol.* 1993;21:604-11.

19. Windberger U, Bartholovitsch A, Plasenzotti R, Korak KJ, Heinze G. Whole blood viscosity, plasma viscosity and erythrocyte aggregationin nine mammalian species: reference values and and comparison of data. *Exp Physiol*. 2003;88:431-40.

20. Vilahur G, Padro T, Badimon L. Atherosclerosis and thrombosis: Insights from large animal models. *J Biomed Biotechnol*. 2011;2011:907575.

21. Schwartz RS, Murphy JG, Edwards WD, Camrud AR, Vliestra RE, Holmes DR. Restenosis after balloon angioplasty. A practical proliferative model in porcine coronary arteries. *Circulation*. 1990;82:2190-200.

22. Staab ME, Srivatsa SS, Lerman A, Sangiorgi G, Jeong MH, Edwards WD, Holmes DR Jr, Schwartz RS. Arterial remodeling after experimental percutaneous injury is highly dependent on adventitial injury and histopathology. *Int J Cardiol*. 1997;58:31-40.

23. Song W, Lee J, Kim H, Shin J, Oh D, Tio F, Wong SC, Hong MK. A new percutaneous porcine coronary model of chronic total occlusion. *J Invasive Cardiol.* 2005;17:452-4.

24. Strauss BH, Goldman L, Qiang B, Nili N, Segev A, Butany J, Sparkes JD, Jackson ZS, Eskandarian MR, Virmani R. Collagenase plaque digestion for facilitating guide wire crossing in chronic total occlusions. *Circulation*. 2003;108:1259-62.

25. Suzuki K, Saito N, Zhang G, Conditt G, McGregor J, Flynn AM, Leahy D, Glennon P, Leon MB, Hayase M. Development of a novel calcified total occlusion model in porcine coronary arteries. *J Invasive Cardiol*. 2008;20:296-301.